Must for candidates of permanent magnet materials

H. Akai
Institute for Solid State Physics, The University of Tokyo, Kashiwa 277-8581, Japan

The basic strategy of designing a new permanent magnet material is to attain a large saturation magnetization M_S, a high Curie temperature T_C, and a strong magnetic anisotropy in a single crystal. The question is then if there are some limits to these quantities and, if it is, what are the values and what determine them. The answer to the first question is "yes". Concerning the second and third questions, obviously the magnetization cannot exceed the local atomic magnetization, which is limited to ~5 μ_B (transition metals) or ~10 μ_B (rare earths) per atomic volume; our experience tells that the possible maximum M_S probably is not larger than 2.5 T that is attained for $Fe_{70}Co_{30}$ alloy (owing to subtle balance between the magnetic moment and volume, see Fig. 1). T_C do not exceed both the intra-atomic coulombic interaction and bandwidth, which could be ~5 eV, being much higher than the melting temperature. Therefore, T_C ~1500 K might be a good estimate of the limit (enough for practical purposes). The magnetic anisotropy originates from the combination of a crystal structure and the spin-orbit coupling. The crystal structure gives rise to a crystal field as well as anisotropy in kinetic energy. The effects could again reach as large as the bandwidth. On the other hand, the strength of the spin-orbit coupling do not exceed ~ 0.1eV even for rare earths. Yet another limitation comes from the exchange coupling: if the atoms that possess a large spin-orbit coupling are different from those carrying magnetic moments, the exchange coupling between those two types of atoms limits the strength of magnetic anisotropy. Eventually, the magnetic anisotropy is limited by the spin-orbit coupling in the case of transition metals and the crystal field (including kinetic part) in the case of rare earths. From such arguments, it may be realistic to define the following figures for an ultimate permanent magnet material: M_S ~ 2.5T, T_C ~1500 K, and K_1 ~ 50 MJ/m^3

In order to realize the above figures to some extent, the following considerations might be helpful: First, the material should be definitely metallic so that the ferromagnetism can be the most stable magnetic structure. For this it is necessary that the main player, Fe, be in a metallic environment. The adding some amount of Co would help to increase M_S and T_C. Moreover, for the ferromagnetic state to be stable, each Fe should take approximately a six coordinate bcc-like structure. In such a situation, high T_C is also guaranteed. Concerning the magnetic anisotropy, it is impossible to attain enough anisotropy with using only transition metal elements: though realizing a highly tetragonal lattice might be possible, the spin orbit coupling will not be strong enough to fix the magnetic moment to the lattice. Then the maximum of K_1 would be ~ 5MJ/m^3. To obtain K_1 one order of magnitude bigger than that definitely needs the existence of rare earths in the system, as is supported by experiences. For example, at law temperature, the magnetic anisotropy of rare earth based permanent magnet materials are mostly comes from rare earth elements. Even at higher temperature where the coupling between Fe and rare earth ions becomes weak, half of the magnetic anisotropy is still owing to the rare earths although the number of rare earth atoms in the unit cell is much smaller than that of Fe atoms.

Further detailed discussion about the must for candidates of permanent magnet materials will be discussed on the basis of first-principles calculation of magnetic and electronic properties of magnetic materials.

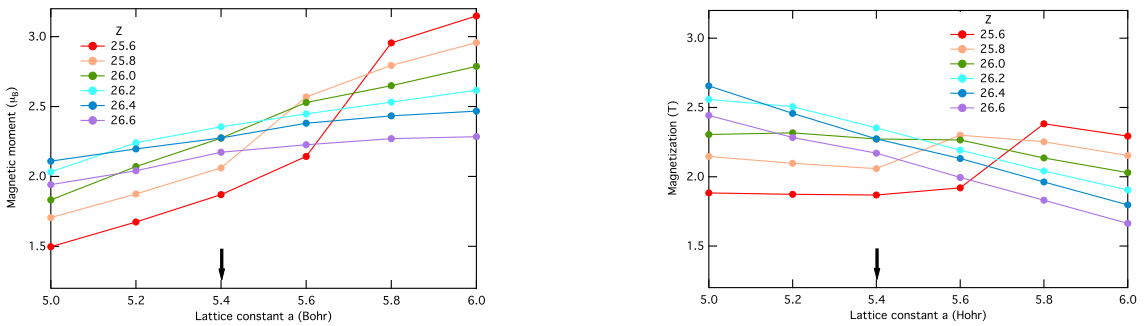

Fig. 1 the magnetic moment (left) and the magnetization M_s as functions of the lattice constant and fictitious nuclear number. The arrows indicate the lattice constant corresponding the minimum of the total energy of the system.

Analysis of magnetic properties for 1-12 rare-earth intermetallics based on first-principles

Takuya Yoshioka, Daiki Suzuki, and Hiroki Tsuchiura
[1]Department of Applied Physics Tohoku University, Sendai 980-8579, Japan
[2]ESICMM, National Institute for Materials Science, Tsukuba 305-0047, Japan

Due to increasing demands for high performance hard magnets for applications like wind turbines or electric vehicles, intensive studies have been carried out to investigate novel magnetic materials with comparable magnetic properties to $Nd_2Fe_{14}B$. Among them, because of high fraction of iron, rare-earth iron intermetallic compounds in ThMn12 structure have attracted constant attention. In particular, the nitrogenated compounds $NdFe_{12}N$ and $NdFe_{11}TiN$ stimulated much more interest among this series of compounds both experimentally and theoretically [1, 2]. The other 1-12 type intermetallics studied by screening approach, where the magnetic properties such as anisotropy fields and maximum energy products are estimated in a systematic way [3].

Motivated by these background, here we focus on *R*Fe12 with *R*=Nd or Sm and investigate their magnetic properties theoretically. First, we calculate the basic magnetic properties such as magnetic moment and magnetic anisotropy of each ion, and then define a crystal field Hamiltonian for *R* ions based on first-principles calculations to construct an effective spin model for these systems. We also carry out the electronic state calculation for these systems with simple surfaces. This is because, we have found that the Nd ions exposed on the (001) surface of the $Nd_2Fe_{14}B$ structure not only lose their uniaxial anisotropy but also exhibit in-plane anisotropy. Here we call such Nd ions as anomalous Nd, and we can expect that the same thing happens also *R*Fe12 systems. Then we carry out spin-dynamics calculations for the effective spin model including the information of surface *R* ions to estimate the expected values of coercivity.

Fig. 1 shows the (001) surface model structure, or the so-called slab model structure, for $NdFe_{12}$ system, as an example. The leading crystal field parameter A20's are shown in the figure. The 1st and 6th Nd ions show the strong c-plane anisotropies. Thus we find that the Nd on the surfaces can be anomalous even for the NdFe12 system. We will also discuss the effects of anormalous *R* (*R*=Nd, Sm) ions for the coercivity in the 1-12 type rare-earth intermetallic compounds.

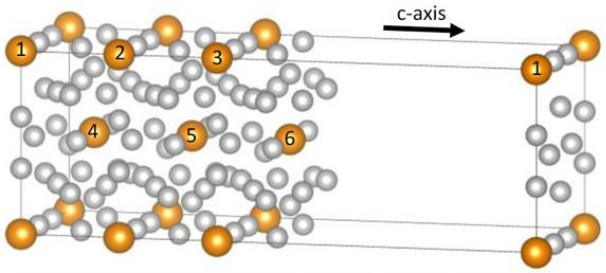

Nd	1	2	3	4	5	6
$A_2^0\langle r^2\rangle$ (K)	-488.4	45.8	-20.9	-8.7	-16.7	-397.0

Fig. 1 Cristal field parameters in NdFe12 surface model

[1] T. Miyake, K. Terakura, Y. Harashima, H. Kino, and S. Ishibashi, J. Phys. Soc. Jpn. **83** (2014) 043702.

[2] Y. Hirayama, Y. K. Takahashi, S. Hirosawa, K. Hono, Scr. Mater. **95** (2015) 70.
[3] W. Körner, G. Krugel, and C. Elsässer, Sci. Rep. 6 (2016) 24686.

The $ThMn_{12}$-type iron rich compounds with high intrinsic magnetic properties as permanent magnet materials

Y. Hirayama[1,2], Y. K. Takahashi[2], S. Hirosawa[2], and K. Hono[2]

1 National Institute of Advanced Industrial Science and Technology

2 Elements Strategy of Initiative Center for Magnetic Materials, National Institute for Materials Science

Iron rich compounds $R{Fe}_{12}(N)_x$ (R: rare earth element) with $ThMn_{12}$ structure is expected to have a high spontaneous magnetization $\mu_0 M_S$, since Fe ratio is highest among known ferromagnetic phases so far. Although $R{Fe}_{12}$ phase is known to be unstable in bulk state, we could demonstrate to prepare $R{Fe}_{12}$ by sputtering process and show higher intrinsic magnetic properties recently[1, 2], as well as the first principles calculation predicted[3]. In this talk, we will introduce how to prepare the $R{Fe}_{12}$ phase and how high potential they have as permanent magnetic materials.

Epitaxial $NdFe_{12}$ and $Sm(Fe_{1-x}Co_x)_{12}$ (x = 0, 0.1 and 0.2) films with 0.35 - 0.65 μm in thickness were prepared on a (001)-oriented W and V underlayer, respectively, deposited on a MgO(001) single crystalline substrate at elevated temperature by a co-sputtering system. Then, for Nd compound, nitriding has been done in nitrogen atmosphere of 1 Pa at 550 °C for 1 hour in order to obtain the uniaxial anisotropy along c axis. The magnetic properties were measured by using SQUID VSM (Quantum Design Inc. MPMS3) and VSM (Quantum Design Inc. DynaCool) in the temperature range of 300 – 700 K with a maximum magnetic field of 7 and 14 T, respectively.

Both $NdFe_{12}N_x$ and $Sm(Fe_{1-x}Co_x)_{12}$ have uniaxial anisotropy along the c-axis which is perpendicular to the MgO(001) plane. Figure 1 showed $\mu_0 M_S$ and $\mu_0 H_A$ against the temperature of $R{Fe}_{12}$ phase together with known ferromagnetic phases. Higher $\mu_0 M_S$ of 1.66 ± 0.08 T and 1.78 ± 0.02 T at 300 K for $NdFe_{12}N_x$ and $Sm(Fe_{0.8}Co_{0.2})_{12}$ were obtained, respectively. Curie temperature T_C was 823K for $NdFe_{12}N_x$ and 555 K for $SmFe_{12}$. By substituting Fe with Co for Sm system, T_C was enhanced with increasing the Co content and reached to 859 K for $Sm(Fe_{0.8}Co_{0.2})_{12}$, which is due to the strong exchange coupling of Fe and Co. This value was by more than 200 K higher than that of $Nd_2Fe_{14}B$. Therefore, these $R{Fe}_{12}$ phases have high potential as permanent magnet materials. The next step should be the investigation to find a way to stabilize the $R{Fe}_{12}$ phase in the bulk state in order to put this phase into practical use.

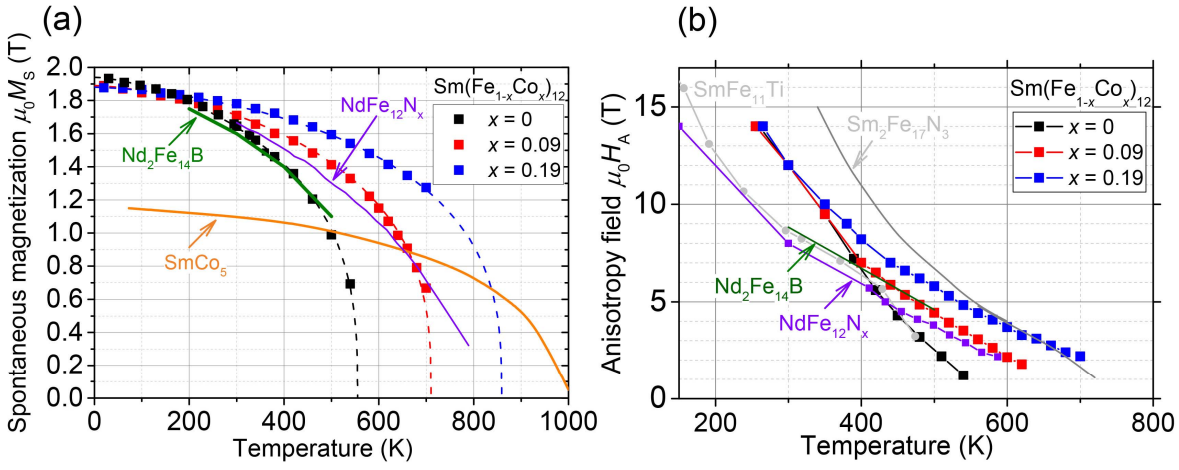

Figure 1 Temperature dependence of (a)spontaneous magnetization and (b)anisotropy field [2] together with known ferromagnetic phases.

Reference

[1] Y. Hirayama *et al.*, *Scripta Materialia* 95 (2015) 70-72. [2] Y.Hirayama *et al.*, *Scripta Materialia* 138 (2017) 62-65.
[3] T. Miyake *et al.*, *Journal of the Physical Society of Japan* 83 (2014) 043702.

High-temperature stability of $ThMn_{12}$ magnet materials

K. Kobayashi[1], D. Furusawa[1], S. Suzuki[1], T. Kuno[1], K. Urushibata[1],
N. Sakuma[2,3], M. Yano[2,3], T. Shoji[2,3], A. Kato[2,3], and A. Manabe[3]
[1] Shizuoka Institute of Science and Technology, Fukuroi 437-8555, Japan
[2] Toyota Motor Corporation, Susono 410-1193, Japan
[3] Technology Research Association of Magnetic Materials for High-efficiency Motors (Mag-HEM)
Higashifuji-Branch, Susono 410-1193, Japan

1. Introduction

We showed that the nitrogenated R = Nd compound $(Nd_{0.7}Zr_{0.3})(Fe_{0.75}Co_{0.25})_{11.5}Ti_{0.5}N_{1.30}$ had good magnetic properties of J_s = 1.67 T and H_a = 5.25 MA/m at room temperature (RT). The R = Sm alloy, $(Sm_{0.8}Zr_{0.2})(Fe_{0.75}Co_{0.25})_{11.5}Ti_{0.5}$, also had J_s = 1.58 T and H_a = 5.90 MA/m at RT. The values in the R = Sm alloy were J_s = 1.50 T and H_a = 3.70 MA/m at 473 K, and were higher than those of the $Nd_2Fe_{14}B$ phase at this temperature [1]-[3]. Because the R = Sm alloy is a Dy-free and N-free powder, it is a promising candidate for sintered magnets. We investigated the site occupation of Nd, Ti, Zr, and Co in these compounds in the $ThMn_{12}$ structure using Cs-corrected scanning transmission electron microscopy [4], [5].

In this study, we studied the high-temperature (700–1300 K) stability of three typical 1-12 compounds, the nitrogenated alloys, $(Nd_{0.7}Zr_{0.3})(Fe_{0.75}Co_{0.25})_{11.5}Ti_{0.5}N_{1.2}$, $Nd(Fe_{0.8}Co_{0.2})_{11}Mo_{1.0}N_{1.0}$, and the non-nitrogenated alloy, $(Sm_{0.8}Zr_{0.2})(Fe_{0.75}Co_{0.25})_{11.5}Ti_{0.5}$. The two nitrogenated compounds were selected because of their high magnetic properties ($-Ti_{0.5}N_{1.2}$) and stability at high temperatures of up to 900 K ($-Mo_{1.0}N_{1.0}$). The third R = Sm alloy was selected for its high magnetic properties at high temperatures [3], and the likelihood that it could be sintered around 1300 K.

In the presentation, we will report about the high temperature stability of above three compounds, but we concentrate our discussion to $(Sm_{0.8}Zr_{0.2})(Fe_{0.75}Co_{0.25})_{11.5}Ti_{0.5}$ compound in this manuscript due to the limitation of space.

2. Experimental and Results

XRD at RT was performed under the following conditions: CuKα: λ = 0.1542 nm; scanning speed, 2θ = 5°/min; sampling, each θ = 0.1°; atmosphere, Ar ($P_{O_2} \approx 10^{-2}$ Pa). The penetration depth of the X-rays (Cu Kα) was estimated to be about 2 μm (similar to the case of α-Fe). The samples were heated at a rate of 10 K/min to each treatment temperature and held at the temperature for 1 h and cooling down, before the XRD measurements at RT. The XRD patterns of the treated samples were indicated in Figure.

We examined the effect of oxidation, which causes the decomposition of $(Sm_{0.8}Zr_{0.2})(Fe_{0.75}Co_{0.25})_{11.5}Ti_{0.5}$ compound (appearance of the α-(Fe, Co) phase), on the stability of the 1-12 phase. The sample was heated at 1073 K in Ar ($P_{O_2} = 10^{-2}$ Pa) and in Ar with oxygen removing by using a ZrO_2 ceramic oxygen pump ($P_{O_2} = 10^{-15}$ Pa; low P_{O_2}) (in figure; 1073K 1h and 1073K 1h low-P_{O_2}, respectively). The temperature increased to 1273 K in the atmosphere also with oxygen removing ($P_{O_2} = 10^{-15}$ Pa; low P_{O_2}) (also in figure; 1273K 1h low P_{O_2}). The

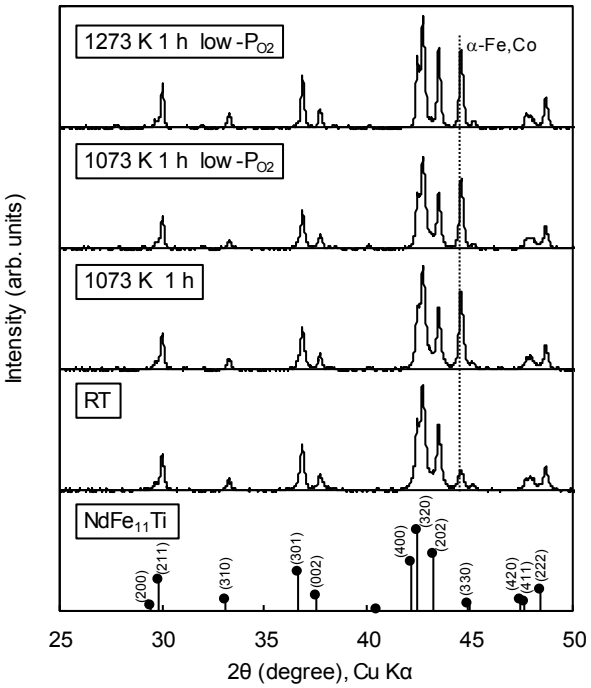

Figure. XRD patterns observed for $((Sm_{0.8}Zr_{0.2})$ $-(Fe_{0.75}Co_{0.25})_{11.5}Ti_{0.5})$. The atmosphere during heat treatment was controlled and measured by using a ZrO_2 ceramic oxygen pump and sensor.

intensities of the strongest peak of the α-(Fe, Co) phase at about 2θ = 44.5° with CuKα diffraction are similar in all treatments as shown in the figure. Therefore, the oxidation was not the main reason for the decomposition of this compound, but heat treatment at >873 K decreased the phase stability.

3. Discussion

From other XRD studies using a high temperature XRD, it was revealed that the $(Sm_{0.8}Zr_{0.2})(Fe_{0.75}Co_{0.25})_{11.5}Ti_{0.5}$ compound decomposed readily in a high PO_2 atmosphere, i.e disappearing of the XRD diffraction peaks of 1-12 phase, that is in the PO_2 was estimated to be >10 Pa [6]. In contrast, the 1-12 structure was stable up to 1273 K at a low PO_2 of 10^{-15} Pa in an Ar atmosphere where oxygen was eliminated by using a ZrO_2 oxygen pump as shown in Figure of this manuscript. Therefore, the oxidation is an important reason of decomposition of the $(Sm_{0.8}Zr_{0.2})(Fe_{0.75}Co_{0.25})_{11.5}Ti_{0.5}$ compound.

Another important characteristic of 1-12 compounds is that the $ThMn_{12}$ structure is stable at high temperatures approximately above 1100 K. Therefore, the $ThMn_{12}$ structure observed by using XRD at RT was a metastable phase. If we heated the structure for several hours at 800–900 K, the structure gradually decomposed into other phases [7]. A characteristic phase appearing after decomposition is the α-Fe phase. When the $(Sm_{0.8}Zr_{0.2})(Fe_{0.75}Co_{0.25})_{11.5}Ti_{0.5}$ compound was heated in a high PO_2 atmosphere, the decomposition was accelerated, although the $ThMn_{12}$ structure was stable up to 1273 K in a low PO_2 of ~10^{-15} Pa as shown in Figure of this manuscript, despite the gradual increase of the (110) peak of the α-Fe phase.

4. Conclusion

The $ThMn_{12}$ phase was metastable at RT, and the samples decomposed at 800–900 K when the samples were kept for long duration, i.e. for several hours. In the case of $(Sm_{0.8}Zr_{0.2})(Fe_{0.75}Co_{0.25})_{11.5}Ti_{0.5}$ compound, the decomposition of the main 1-12 phase was accelerated by the oxidation that occurred under a high PO_2 atmosphere as PO_2 > 10 Pa. Conversely, the main phase was stable up to, and should be more than, 1273 K in a low PO_2 of ~10^{-15} Pa.

Acknowledgment

This study is based on results obtained from the future pioneering program “Developments of magnetic materials technology for high efficiency motors” commissioned by the New Energy and Industrial Technology Development Organization (NEDO).

Reference

1) S. Suzuki, T. Kuno, K. Urushibata, K. Kobayashi, N. Sakuma, K. Washio, H. Kishimoto, A. Kato and A. Manabe, A $(Nd,Zr)(Fe,Co)_{11.5}Ti_{0.5}N_x$ compound as a permanent magnet material, AIP Advances 4 (2014) 117131.
2) N. Sakuma, S. Suzuki, T. Kuno, K. Urushibata, K. Kobayashi, M. Yano, A. Kato and A. Manabe, Influence of Zr substitution on the stabilization of $ThMn_{12}$-type $(Nd_{1-\alpha}Zr_{\alpha})(Fe_{0.75}Co_{0.25})_{11.25}Ti_{0.75}N_{1.2-1.4}$ (α = 0–0.3) compounds, AIP Advances 6 (2016) 056023.
3) T. Kuno, S. Suzuki, K. Urushibata, K. Kobayashi, N. Sakuma, M. Yano, A. Kato and A. Manabe, $(Sm,Zr)(Fe,Co)_{11.0\text{-}11.5}Ti_{1.0\text{-}0.5}$ compounds as new permanent magnet materials, AIP Advances 6 (2016) 025221.
4) K. Kobayashi, S. Suzuki, T. Kuno, K. Urushibata, N. Sakuma, M. Yano, A. Kato and A. Manabe, Proc. of REPM2016, Darmstadt, Germany, (2016) O4-1645,
5) K. Kobayashi, S. Suzuki, T. Kuno, K. Urushibata, N. Sakuma, M. Yano, A. Kato and A. Manabe, J. Alloys and Compounds, 694 (2017) pp.914-920.
6) K. Kobayashi et al., will be published in Thermochimica Acta.
7) V. Raghavan, J. Phase Equlibria, vol.21 No.5 (2000) pp.464-466.

Coercivity dependence on particle size in three $ThMn_{12}$-type magnetic materials

T. Kuno[1], K. Muramatsu[1], S. Suzuki[1], K. Urushibata[1], K. Kobayashi[1],
N. Sakuma[2,3], A. kinoshita[2,3], K. yokota[2,3], M. Yano[2,3], T. Shoji[2,3], A. Kato[2,3], A. Manabe[3]
[1]Shizuoka Institute of Science and Technology, Fukuroi, 437-8555, Japan
[2]Toyota Motor Corporation, Susono, 410-1193, Japan
[3]Technology Research Association of Magnetic Materials for High-efficiency Motors (Mag-HEM)
Higashifuji-Branch, Susono, 410-1193, Japan

Introduction

We found $RFe_{11-x}M_x$ (R=Nd,Sm) compounds having a $TnMn_{12}$ type structure as new magnet materials showing magnetic properties exceeding $Nd_2Fe_{14}B$ magnet at room temperature (RT). Typical examples of the compounds are $(Nd_{0.7}Zr_{0.3})(Fe_{0.75}Co_{0.25})_{11.5}Ti_{0.5}N_{1.3}$ [1) 2)] and sinterable $(Sm_{0.8}Zr_{0.2})(Fe_{0.75}Co_{0.25})_{11.5}Ti_{0.5}$ [3)]. Furthermore, it was revealed that the anisotropy magnetic field (H_a) of $Nd(Fe_{0.8}Co_{0.2})_{11}Mo$ nitrides in which the third component element is Mo has a high value of H_a=8.95 MA/m at RT. In this study, the improvement of coercivity (H_c) by decreasing particle size will be studied for the purpose of realizing the usable industrial magnets by the compounds.

Experimental method

We will report the results of Mo based compound in this manuscript. The $Nd(Fe_{0.8}Co_{0.2})_{11}Mo$ alloy prepared by the strip cast (SC) method was subjected to annealing at 1100°C/4 hours (h) and then pulverized and classified to prepare a powder sample having a particle size < 32 μm. The powder sample was nitrided in N_2 gas atmosphere at 600 °C/4 h, and the obtained $Nd(Fe_{0.8}Co_{0.2})_{11}MoN_{1.1}$ nitride was refined by ball mill grinding. Ball mill pulverization was carried out using stainless steel balls having a diameter of 3mmφ at a rotation speed of 180 to 300 rpm for 0 - 40 h in cyclohexane solvent.

The average particle diameter (D_{AVE}) of the powder sample was measured by scanning electron microscope (SEM) observation of the particle areas of about 100 particles and converted into particle diameters. The magnetic properties were measured using a 5T-VSM (manufactured by Toei Kogyo Co., Ltd.) and the oxygen content (wt.%) of the powder samples were measured by gas analysis (TC-436AR, manufactured by LECO Co., Ltd.) by inert gas melting method.

Experimental result

Figure 1 shows the SEM images of $Nd(Fe_{0.8}Co_{0.2})_{11}MoN_{1.1}$ nitride before and after ball mill grinding. By ball mill grinding 40 h, D_{AVE} of the same powder sample was refined from D_{AVE} =14.1 μm (0 h) to D_{AVE} =1.4 μm (40 h).

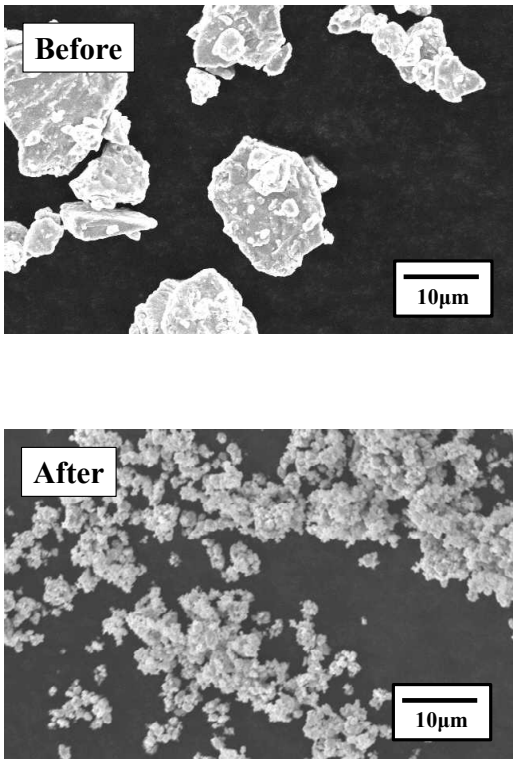

Fig. 1 $Nd(Fe_{0.8}Co_{0.2})_{11}MoN_{1.1}$ nitride before and after grinding (grinding time 40 h).

Fig. 2 shows the relationship between D_{AVE} and H_c, and oxygen contents (wt.%) of the same powder samples. H_c of the powder sample reached to the maximum value of H_c=2.4 kOe (D_{AVE} =1.7 μm) with milling for 16 h and decreased to H_c=2.1 kOe for 40 h. Since the oxygen contents (wt.%) by gas analysis of the powder samples were H_c=2.4 kOe (1.7 wt.%) and H_c=2.1 kOe (3.6 wt.%) respectively, the decrease in H_c in the latter powder should be due to oxidation.

In presentation, we will report similar H_c improvement by refining the sinterable R=Sm based compound and R=Nd based nitride.

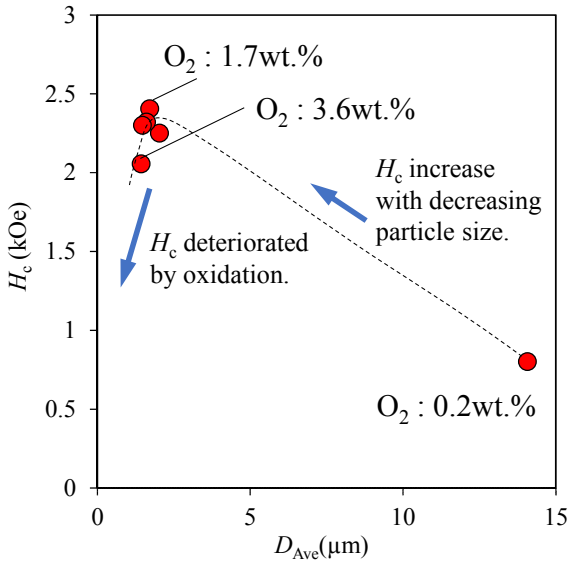

Fig. 2 H_c change with decreasing of D_{AVE}, and oxygen contents in $Nd(Fe_{0.8}Co_{0.2})_{11}MoN_{1.1}$ nitride.

Acknowledgment

This study is based on results obtained from the future pioneering program "Developments of magnetic materials technology for high efficiency motors" commissioned by the New Energy and Industrial Technology Development Organization (NEDO).

Reference

1) S. Suzuki et al., AIP Advances, 4 (2014)
2) S. Suzuki et al., J. Magn. Magn. Mater., 401 (2016) 259-268.
3) T. Kuno, et al., AIP Advances, 6 (2016) 025221.

Nd-Fe-B permanent magnets with ultimate hard magnetic properties

K. Hono, H. Sepehri-Amin, T. T. Sasaki, and T. Ohkubo
Elements Strategy Initiative Center for Magnetic Materials, National Institute for Materials Science (NIMS), Tsukuba, Japan

Due to the recent concern about the stable supply of heavy rare earth elements, attaining high coercivity in Nd-Fe-B magnets without using heavy rare earth (HRE) elements has received intense research interest in the past decade. However, the supply of rare earth elements has been stabilized in the last few years, and the renewed goal is to how to achieve the highest permanent magnetic properties with a balanced use of critical elements. In this talk, we will overview our recent progresses carried out at NIMS in collaboration with many industrial partners that were carried out toward the development of high coercivity Dy-free Nd-Fe-B permanent magnets. Thereafter, we discuss how to achieve ultimate permanent magnet properties with trace additions of HRE. To obtain better understandings of the microstructure-coercivity relationships, we investigated the microstructures of experimental Nd-Fe-B sintered magnets, those processed from HDDR power, and hot-deformed magnets with different values of coercivity depending on chemical compositions, processing routes and post-manufacturing heat treatments. The microstructure and magnetic domain observations have been carried out using aberration-corrected STEM, atom probe tomography (APT), magneto-optical Kerr microscopy and finite element micromagnetic simulations. We found that the intergranular phase parallel to the c-planes are mostly crystalline with a higher Nd concentration in contrast to that lying parallel to the c-axis that contains higher Fe content with an amorphous structure in both sintered and hot-deformed magnets. Micromagnetic simulations suggest the reduction of the magnetization in the latter is critical to enhance the coercivity. Based on these new experimental findings together with our detailed characterization results of the intergranular phases in Ga-doped Nd-Fe-B magnets, we developed a method to increase the coercivity of Nd-Fe-B hot-deformed magnets while keeping relatively high remanence.

This talk includes results obtained in collaboration with industrial collaborators including TOYOTA, Toyota Central Research Lab. Intermetallics and Daido Steel conducted under CREST and Collaborative Research Based on Industrial Demand projects.

Large scale micromagnetic simulation and analysis of magnetization reversal within hot-deformed permanent magnet

H. Tsukahara[1], K. Iwano[1], C. Mitsumata[2], T. Ishikawa[1], K. Ono[1]
[1]High Energy Accelerator Research Organization (KEK), Tsukuba, Ibaraki 305-0801, Japan
[2]National Institute for Materials Science (NIMS), Tsukuba 305-0047, Japan

Introduction

The hot-deformed permanent magnet is one of the promising material for high coercivity and a remanent magnetization that are necessary for high-efficiency power motors. This permanent magnet consists of many tabular grains that interact with each other through exchange and dipole interaction. The interaction among the grains propagates magnetization reversal across the grain interface during demagnetization process. Thus, it is important for a further high-performance permanent magnet to reveal how the magnetization reversal propagates within the permanent magnet. In this study, we performed large-scale micromagnetic simulation using our simulation code [1] based on Landau–Lifshitz–Gilbert equation and analyzed simulation data to clarify magnetization reversal process inside the hot-deformed magnet.

Model and method

Figure 1(a) shows the simulation model of a nanocrystalline hot-deformed permanent magnet of size 1024 nm × 1024 nm × 512 nm. This model is created by stacking the layers that consist of the tabular grain with an average diameter of 160 nm and thickness 32 nm. Directions of the easy axis of the grains tilt from the z axis with the average axial inclination 11.6°. We discretized the simulation model into 2.0 nm × 2.0 nm × 2.0 nm. Thus, we use about 0.3 billion calculation cells for our simulation, and the simulation model has the 3,384 tabular grains. The following $Nd_2Fe_{12}B$ material parameters are assumed in our simulation: saturation magnetization 1281.2 emu/cm^3, uniaxial constant 4.5×10^7 erg/cm^3, exchange stiffness constant 12.5×10^{-7} emu/cm^3, and Gilbert damping constant 1.0. We choose 12.5×10^{-9} emu/cm^3 for inter-grain exchange interaction.

Results

Figure 1(b) shows the calculated hysteresis curve. The coercivity of our simulation model is 29.0 kOe. When an external field exceeds 28.0 kOe, nucleation cores occur in some grains, and the magnetization reversal propagates across the grain interface. Figure 1(c) shows the magnetization structure in the each grain as a function a grain diameter and tilt angle of the easy axis when the nucleation cores appear. The nucleation core tends to be created in the grain whose tilt angle is about 30° (blue circle). The magnetization reversal propagates across the grain interface and, finally, the interaction domain structure appears. However, the distribution of the grain in which the magnetization reverses (green circle) is almost same that of the grains in which magnetization does not reverse (red circle) as shown in Fig. 1(d). In this presentation, we will talk about details of the propagation of the magnetization reversal between the grains.

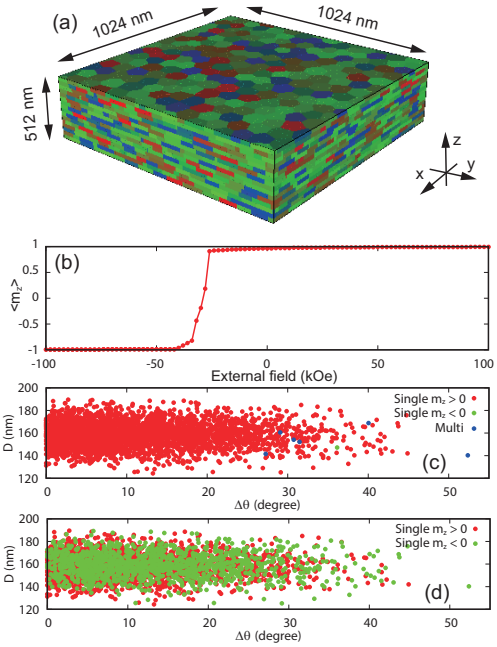

Fig 1: The illustration of the simulation model (a), the calculated hysteresis curve (b), and (c) the magnetization structure of the each grain when the nucleation core occur (c), and the interaction domain is created (d).

Acknowledgments

The simulation were performed by the Large Scale Similation Program 15/16-18 of KEK.

[1] H. Tsukahara, K. Iwano, C. Mitsumata, T. Ishikawa, K. Ono, Comput. Phys. Commun, 207, 217 (2016).

Proposal for coercivity mechanism in rare-earth magnets based on comparison between experiments on model-interface samples and ab-initio calculations

H. Kato, K. Koike, D. Ogawa, M. Itakura* and Y. Ando**
(Yamagata Univ., *Kyushu Univ., **Tohoku Univ.)

There are high needs of developing higher coercivity Nd-Fe-B magnets without using heavy rare elements. In our project research, our final goal is to obtain a guiding principle to create supreme-performance permanent magnets beyond that of the current Nd-Fe-B magnet, by making full use of the nanoscale structure control to create the model-interface samples, which simulate the intergranular structure of sintered Nd-Fe-B magnets. We investigate the magnetic properties of these model-interface samples and compare the experimental results with the ab-initio calculations.
We briefly describe the results of our project research below and propose a hypothesis for the coercivity mechanism dominated in sintered Nd-Fe-B magnets.

(1) Effect of Nd and La coating on the coercivity of highly-oriented $Nd_2Fe_{14}B$ thin films

Highly oriented $Nd_2Fe_{14}B$ thin films were fabricated on the single-crystal substrates, with the *c*-axis of the tetragonal $Nd_2Fe_{14}B$ cell perpendicular to the film plane. As the average grain size was decreased from 300 nm to 50 nm, the coercivity H_c increased linearly from 7 kOe to 17 kOe, as shown by the black circles in Fig. 1. We then coated these films with the Nd overlayer and annealed, which led to the systematic enhancement of the coercivity [1] as shown by the red circles in the Fig. 1. Similar behavior was observed for the La-coated $Nd_2Fe_{14}B$ films [2] as shown by the cross symbols in Fig.1. Detailed microstructure investigation on these samples have shown us that there exist the oxide phases of Nd or La at the interface with the $Nd_2Fe_{14}B$ phase in both of the two model systems. In the sintered Nd-Fe-B magnets, we recognized so far that an existence of the excess Nd in the vicinity of the main $Nd_2Fe_{14}B$ phase was crucial for the higher coercivity based on the morphology change of the Nd-rich phase after low-temperature annealing [3]. However, the results shown in Fig. 1 strongly suggest that it is not the Nd nor the La but the O atom, that is important for the coercivity enhancement. We then performed recently the atomic-scale investigation of the interface structure in the La-coated $Nd_2Fe_{14}B$ films before (H_c~10 kOe) and after (H_c~15 kOe) annealing. The STEM-EDS elemental analysis revealed that the content of La, Nd, and Fe was unchanged by the annealing, and showed that the only difference caused by the annealing was the O content in the LaO_x layer, which increased from 15 to 35 at.% [4]. These results therefore suggest that the magnetocrystalline anisotropy of the Nd atoms which would be reduced at the surface of $Nd_2Fe_{14}B$ has then recovered by a presence of O, leading to a remarkable enhancement of the coercivity. This discovery is in consistent with the recent theoretical calculation reported by Toga et al.[5].

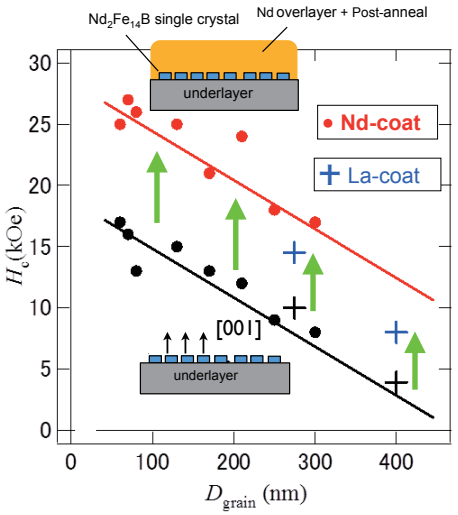

Fig. 1 Coercivity of Nd- and La-coated $Nd_2Fe_{14}B$ films after post annealing, together with that for the uncoated $Nd_2Fe_{14}B$ films, as a a function of averaged grain size along the lateral direction.

(2) Orientation-dependent exchange coupling between $Nd_2Fe_{14}B$ and α-Fe interfaces

An idea of exchange-coupled hard/soft nanocomposite magnets is the promising candidate [6] to fabricate superior-performance magnets exceeding the theoretical limit of the energy-product value in the Nd-Fe-B magnet. In the case of $Nd_2Fe_{14}B/\alpha$-Fe

system, reported $(BH)_{max}$ values are still much lower because of the difficulty in controlling the size and alignment of the hard-phase grains. Moreover, the exchange coupling between the hard and soft magnetic phases is the important factor in dominating the magnetic properties of the nanocomposite magnet. Being motivated by the stimulating theoretical prediction [7], a model sample with an interface of the $Nd_2Fe_{14}B(100)$ plane and the α-Fe were fabricated in order to evaluate the exchange-coupling constant J_{ex} between these two ferromagnetic phases. By measuring the ferromagnetic resonance fields and the Kerr loops, the exchange-coupling constant J_{ex} was confirmed to be negative [8] with the value of $J_{ex} = -6.5\times10^{-4}$ J·m^{-2} at the $Nd_2Fe_{14}B(100)$/α-Fe interface, in striking contrast to the positive J_{ex} value for the $Nd_2Fe_{14}B(001)$/α-Fe interface [9, 10]. Figure 2 shows the field-induced moment reversal behavior of the Fe magnetic moment, which is the direct evidence of the antiparallel coupling at zero field, i. e. the negative J_{ex}.

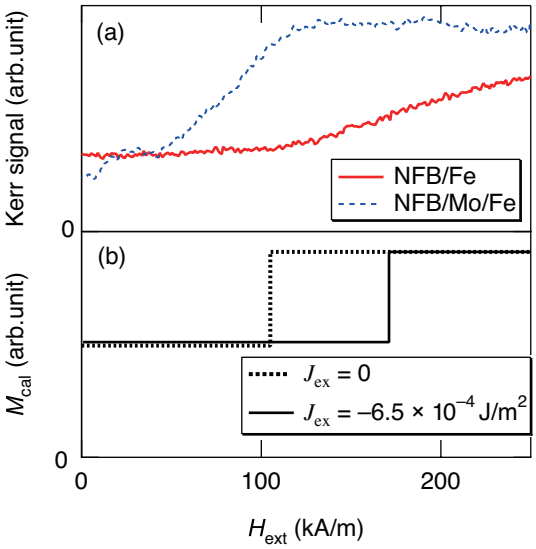

Fig. 2 (a) Local magnetization curves measured by longitudinal MOKE in $Nd_2Fe_{14}B(100)$/α-Fe and $Nd_2Fe_{14}B(100)$/Mo/α-Fe samples, in comparison with (b) the calculated magnetization curves with and without negative exchange coupling. Field-induced spin-flip transition indicates the antiparallel exchange coupling at the interface in the $Nd_2Fe_{14}B(100)$/α-Fe sample.

Other topics to be introduced in the presentation are as follows.

(3) Surface state and spin switching in millimeter-sized single crystals of $R_2Fe_{14}B$ (R=Nd and Tb)

(4) Creation of orientation-controlled $Nd_2Fe_{14}B$/α-Fe nano-composite magnets

We finally propose a hypothesis that an existence of not only the O but also Fe or Cu at the interface is essential [5, 11] for the recovery of the magnetocrystalline anisotropy of the R atoms which would have been reduced being at the outermost surface of the $R_2Fe_{14}B$ grains owing to a breaking of the periodic symmetry. This scenario would be applicable to other rare-earth-containing permanent magnets, provided that a nucleation of reversed domains is the dominant process for the coercivity. This work was supported by the Collaborative Research Based on Industrial Demand, from Japan Science and Technology Agency (JST).

References

[1] K. Koike, T. Kusano, D. Ogawa, K. Kobayashi, H. Kato, M. Oogane, T. Miyazaki, Y. Ando and M. Itakura, Nano. Res. Lett., (2016) 11:33.

[2] K. Koike, H. Ishikawa, D. Ogawa, H. Kato, T. Miyazaki, Y. Ando, and M. Itakura, Physics Procedia, 75 (2015) 1294.

[3] F. Vial, F. Joly, E. Nevalainen, M. Sagawa, K. Hiraga, and K. T. Park, J. Magn. Magn. Mater., 242-245 (2002)1329.

[4] M. Itakura, J. Fukuda, K. Koike, H. Ishikawa, D. Ogawa, and H. Kato, AIP Advances, 7 (2017) 035301-1-9.

[5] Y. Toga, T. Suzuki, and A. Sakuma, J. Appl. Phys., 117 (2015) 223905-1.

[6] E. F. Kneller and R. Hawig, IEEE Trans. Magn., 27 (1991) 3588.

[7] Y. Toga, H. Moriya, H. Tsuchiura and A. Sakuma, J. Phys.: Conf. Series, 266 (2011) 012046-1.

[8] D. Ogawa, K. Koike, S. Mizukami, T. Miyazaki, M. Oogane, Y. Ando, and H. Kato, Appl. Phys. Lett., 107 (2015) 102406.

[9] D. Ogawa, K. Koike, S. Mizukami, M. Oogane, Y. Ando, T. Miyazaki and H. Kato, J. Magn. Soc. Jpn., 36 (2012) 5.

[10] D. Ogawa, K. Koike, S. Mizukami, T. Miyazaki, M. Oogane, Y. Ando, and H. Kato, J. Kor. Phys. Soc., 63 (2013) 489.

[11] S. Tanaka, H. Moriya, H. Tsuchiura, A. Sakuma, M. Divis, and P. Novak, J. Appl. Phys., 109 (2011) 07A702-1.

Angular Dependence of Coercivity Derived from Alignment Dependence of Coercivity in Sintered Nd-Fe-B Magnets

Yutaka Matsuura[1], Tetsuya Nakamura[2], Kazushi Sumitani[2], Kentaro Kajiwara[2], Ryuji Tamura[3], Kozo Osamura[1]
([1] Research Institute of Applied Sciences, Kyoto 606-8202, Japan; [2] Japan Synchrotron Radiation Research Institute, SPring-8, Kouto Sayo 679-5198 Japan; [3] Tokyo University of Science, Tokyo 125-8585, Japan)

The coercivity of Nd-Fe-B sintered magnets and ferrite magnets decreases as the alignment (α=Br/Js) improves. It was found that their coercivity reaches 70% of that of istropically oriented magnets at the perfect alignment (α=1). [1] These results could not be explained by the coherent rotation model, but they were qualitatively explained by the magnetic domain wall motion model. The angular dependence of coercivity is usually used to verify which model is suitable for the coercivity mechanism. But, it is difficult to decide.

Magnets of several different compositions were made by the powder metallurgical method that is described in our previous papers. [2] To investigate the alignment dependence of coercivity, we used $Nd_{13.48}Co_{0.55}B_{5.76}Fe_{bal.}$ with α=0.95 and $Nd_{12.75}Dy_{0.84}B_{5.81}Co_{0.55}Fe_{bal.}$ for anisotropically aligned magnets. For the angular dependence of coercivity of anisotropically aligned magnets, we used $Nd_{14.2}B_{6.2}Co_{1.0}Fe_{bal.}$ and $Nd_{14.2}Dy_{0.3}B_{6.2}Co_{1.0}Fe_{bal.}$, which have similar compositions to analyze the alignment dependence of coercivity. Coercivity was measured by permeameter. Samples and the measurement method used for the angular dependence of coercivity are mentioned in our previous papers. [2]

Figure 1 shows the observed alignment dependence of the coercivity change rate obtained from that of isotropically oriented magnets, and the calculation results that were obtained using the statistical method based on the Gaussian distribution, which served as the alignment distribution. In the calculation results, we used the postulation that every grain follows the 1/cos θ law. It was found that the calculated curve differed from the observed curve. Figure 2 shows the magnetization reversed area. The solid curve is the calculation result obtained from the same method as Fig. 1. The magnetization reversed areas of $Nd_{12.75}Dy_{0.84}B_{5.81}Co_{0.55}Fe_{bal.}$ and $Nd_{14.2}Dy_{0.3}B_{6.2}Co_{1.0}Fe_{bal}$ are 30° and 36°, which was wider than the expected values for their alignment distributions. We used 30° and 36° along the solid line in Fig. 2, which have 31° and 44° for as the standard deviations of the Gaussian distribution, and applied them to the calculation of the angular dependence of coercivity.

Figure 3 shows the observed angular dependence of $Nd_{14.2}B_{6.2}Co_{1.0}Fe_{bal.}$ and $Nd_{14.2}Dy_{0.3}B_{6.2}Co_{1.0}Fe_{bal.}$, and the calculation results. It was found that the calculation results qualitatively explain the observed angular dependence of coercivity. These results reinforce our conclusion that the magnetic domain wall is pinned at grain tilted away from the easy magnetization direction, and when the magnetic domain wall de-pinned from the pinning sites, the magnetic domain wall jump through several grains, which means that the crust of the grain reverse because of the magnetic domain wall jump.

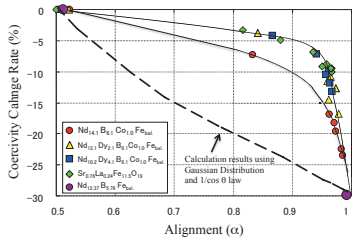

Fig.1 Alignment dependence of coercivity change rate

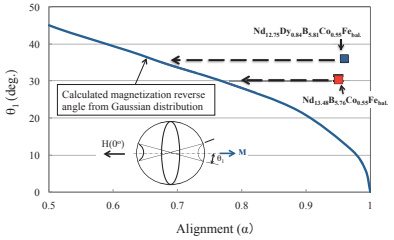

Fig.2 Alignment dependence of magnetization reverse area

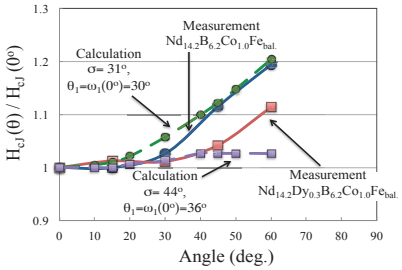

Fig. 3 Angular dependence of coercivity

References

1) Y. Matsuura, R. Ishii, J. Hoshijima, J. Magn. Magn. Mater. 336 (2013) 88
2) Y. Matsuura, N. Kitai, R. Ishii, M. Natsumeda, J. Hoshijima, F. Kuniyoshi, J. Magn. Magn. Mater. 398 (2016) 246